Sigma Receptor 1 Modulates Endoplasmic Reticulum Stress in Retinal Neurons

Yonju Ha,[1] *Ying Dun,*[1] *Muthusamy Thangaraju,*[2] *Jennifer Duplantier,*[1] *Zheng Dong,*[1] *Kebin Liu,*[2] *Vadivel Ganapathy,*[2] *and Sylvia B. Smith*[1,3]

Purpose. To investigate the mechanism of σ receptor 1 (σR1) neuroprotection in retinal neurons.

Methods. Oxidative stress, which is implicated in diabetic retinopathy, was induced in mouse primary ganglion cells (GCs) and RGC-5 cells, and the effect of the σR1 ligand (+)-pentazocine on pro- and anti-apoptotic and endoplasmic reticulum (ER) stress gene expression was examined. Binding of σR1 to BiP, an ER chaperone protein, and σR1 phosphorylation status were examined by immunoprecipitation. Retinas were harvested from *Ins2*$^{Akita/+}$ diabetic mice treated with (+)-pentazocine, and the expression of ER stress genes and of the retinal transcriptome was evaluated.

Results. Oxidative stress induced the death of primary GCs and RGC-5 cells. The effect was decreased by the application of (+)-pentazocine. Stress increased σR1 binding to BiP and enhanced σR1 phosphorylation in RGC-5 cells. BiP binding was prevented, and σR1 phosphorylation decreased in the presence of (+)-pentazocine. The ER stress proteins PERK, ATF4, ATF6, IRE1α, and CHOP were upregulated in RGC-5 cells during oxidative stress, but decreased in the presence of (+)-pentazocine. A similar phenomenon was observed in retinas of *Ins2*$^{Akita/+}$ diabetic mice. Retinal transcriptome analysis of *Ins2*$^{Akita/+}$ mice compared with wild-type revealed differential expression of the genes critically involved in oxidative stress, differentiation, and cell death. The expression profile of those genes was reversed when the *Ins2*$^{Akita/+}$ mice were treated with (+)-pentazocine.

Conclusions. In retinal neurons, the molecular chaperone σR1 binds BiP under stressful conditions; (+)-pentazocine may exert its effects by dissociating σR1 from BiP. As stress in retinal cells increases, phosphorylation of σR1 is increased, which is attenuated when agonists bind to the receptor. (*Invest Ophthalmol Vis Sci.* 2011;52:527–540) DOI:10.1167/iovs.10-5731

Sigma (σ) receptors comprise a unique, pharmacologically defined, non-opioid family of proteins that bind psychotropic agents from many structural classes.[1,2] σR1 is expressed ubiquitously and has been cloned in several species.[3–6] The endogenous function of σR1 is not known, but ligands for the receptor have been shown to decrease pain, enhance memory, and promote neuroprotection.[1] Classes of compounds that bind σR1 include benzomorphans ((+)-SKF-10047, (+)-pentazocine, and (+)-3-PPP), antipsychotics (haloperidol, spiperone), antidepressants (imipramine), and neurosteroids (progesterone, testosterone).[2] The σ_1 receptor is distinct from the σ_2 receptor, in that it exhibits high affinity and stereoselectivity for the (+)-isomers of pentazocine, SKF 10047, cyclazocine, and 1-phenylcyclohexanecarboxylate hydrochloride (PRE-084). Other compounds such as haloperidol and eliprodil bind σR1 but also bind other receptors, such as D2 and NMDA receptors, respectively. Compounds that are marketed as antagonists of the site include BD1047 and NE 100 hydrochloride. The neuroprotective effects of ligands for σR1 have been reported, not only in the brain[7,8] but also in the retina.[9–14]

The mechanism of σR1-mediated neuroprotection is unknown; studies suggest that σR1 acts at the mitochondria-associated endoplasmic reticulum (ER) membrane.[15] σR1 has been localized to the ER membrane in NG108-15 cells.[16] We localized σR1 to the ER and nuclear membranes of retinal Müller glial cells.[17] The ER is the entry site for proteins into the secretory pathway. Proteins are translocated into the ER lumen in an unfolded state and require protein chaperones and catalysts of protein folding to attain their final appropriate conformation.[18,19] A sensitive system prevents misfolded proteins from progressing through the secretory pathway and directs them toward a degradative pathway.

The processes that prevent accumulation of unfolded proteins in the ER lumen are regulated by an intracellular signaling pathway known as the unfolded protein response (UPR). The UPR facilitates cellular adaptation to alterations in protein-folding in the ER lumen by expanding the capacity for protein folding. This expansion is accomplished by molecular chaperone proteins such as BiP (a 78-kDa glucose-regulated protein also known as GRP78), calreticulin, and calnexin. When unfolded proteins accumulate in the ER, resident chaperones (such as BiP) release transmembrane ER proteins (e.g., PERK, IRE1, and ATF6) that induce the UPR. Persistent protein misfolding initiates apoptosis and plays a fundamental role in disease pathogenesis of diabetes, atherosclerosis, and neurodegenerative disorders.[18,19]

ER stress is implicated in the pathogenesis of diabetic retinopathy.[20–22] Li et al.[23] reported increased levels of BiP (GRP78), IRE1α, and PERK in the retinas of *Ins2*$^{Akita/+}$ diabetic mice. The *Ins2*$^{Akita/+}$ mouse[24] has been shown to undergo marked apoptosis of retinal neurons, including ganglion cells (GCs) and cells of the inner nuclear layer.[11,25,26] Another key role of the ER is control of Ca^{2+} homeostasis; it supplies Ca^{2+} directly to mitochondria via inositol 1,4,5-triphosphate receptors (IP_3Rs). Mitochondria act as a spatial Ca^{2+} buffer that reduces cytosolic Ca^{2+} overload; σR1-agonists enhance IP_3R-dependent Ca^{2+} release from the ER.[27] Interestingly, when Ca^{2+} stores are depleted, σR1s are redistributed from the mitochondria-associated ER membrane to the entire ER network. In vitro studies provide evidence that σR1 forms a

From the Departments of [1]Cellular Biology and Anatomy, [2]Biochemistry and Molecular Biology, and [3]Ophthalmology, Medical College of Georgia, Augusta, Georgia.

Supported by National Institutes of Health Grant R01 EY014560.

Submitted for publication April 19, 2010; revised June 15 and July 30, 2010; accepted August 17, 2010.

Disclosure: **Y. Ha**, None; **Y. Dun**, None; **M. Thangaraju**, None; **J. Duplantier**, None; **Z. Dong**, None; **K. Liu**, None; **V. Ganapathy**, None; **S.B. Smit**, None

Corresponding author: Sylvia B. Smith, Department of Cellular Biology and Anatomy, Medical College of Georgia, 1459 Laney Walker Boulevard, CB 2820, Augusta, GA 30912-2000; sbsmith@mail.mcg.edu.

complex with the molecular chaperone BiP in Chinese hamster ovary (CHO) cells.[15] Agonists for the receptors have been shown to free σR1 from BiP. Owing to the role of σR1 in regulating Ca^{2+} channels[13,14] and the effects of Ca^{2+} depletion on subcellular location of σR1, these receptors have been defined as Ca^{2+}-sensitive, ligand-mediated molecular chaperones. No studies of the role of σR1 in counteracting ER stress in retina or mitigating the UPR in the retina have been reported. In this study, we noted increased ER stress gene expression in in vitro models of retinal neuronal death induced by oxidative stress and recorded similar trends in vivo in the retinas of *Ins2*$^{Akita/+}$ diabetic mice, which was reversed by treatment with (+)-pentazocine (PTZ). We also observed increased binding of σR1 to BiP and increased phosphorylation of serine in σR1 subsequent to cellular stress.

Materials and Methods

Animals and Cell Culture

Primary ganglion cells (primary GCs) were isolated from the retinas of ~1- to 5-day-old C57BL/6 mice, according to our published method[10]; verification of cell purity has been reported.[28,29] The RGC-5 cell line,[30] recently shown to be a mouse neuronal precursor cell line,[31] was maintained in DMEM:F12, supplemented with 10% FBS, 100 U/mL penicillin, and 100 μg/mL streptomycin. Experiments using the C57Bl/6-*Ins2*$^{Akita\pm}$ mice, including the dosage regimen of (+)-PTZ (dosage: 0.5 mg kg^{-1} twice a week IP; Sigma-Aldrich Corp., St. Louis, MO;) followed previously described methods.[11] Care and use of mice adhered to the guidelines in the ARVO Statement for the Use of Animals in Ophthalmic and Vision Research. Weights and blood glucose levels of the mice are provided (Table 1).

TUNEL Assay

Primary GCs were exposed for 18 hours to xanthine:xanthine oxidase (X:XO; 10 μM:2 mU/mL) in the presence or absence of (+)-PTZ (3 μM). TUNEL analysis was performed (ApopTag Fluorescein In Situ Apoptosis Detection Kit; Chemicon, Temecula, CA), per the manufacturer's instructions. Three coverslips were prepared per treatment; images were captured from five fields (AxioVision software system; Carl Zeiss Meditec, Inc., Dublin, CA). The number of cells emitting the green fluorescence indicative of apoptosis was counted. Data are expressed as apoptotic cells per total number of cells in the field (the nuclei of which were visualized by Hoechst stain 33342, which emits blue fluorescence when bound to dsDNA). Companion experiments were performed in which cells were examined by differential interference contrast (DIC) microscopy, to analyze neuronal projections.[10]

Xanthine Oxidase Assay

A xanthine oxidase assay was performed per the manufacturer's instructions (Xanthine Oxidase Assay Kit; BioVision, Mountain View, CA) to examine whether (+)-PTZ would interact directly with the oxidative stressor used in the experiments. Xanthine oxidase oxidizes xanthine to form hydrogen peroxide (H_2O_2), which reacts stoichiometrically with a colorimetric substrate probe (OxiRed; BioVision) to generate a detectable color at $\lambda = 570$ nm. Using the reagents provided in the kit, we generated a hydrogen peroxide standard curve and used it to calculate the H_2O_2 produced by various concentrations of X:XO. X:XO was prepared at two concentrations (25 μM:10 mU/mL and 10 μM:2 mU/mL) in buffer in the presence or absence of (+)-PTZ (3 μM).

Semiquantitative and Real-Time Quantitative RT-PCR Analysis for Genes in the Pro- and Anti-apoptotic Pathways and the ER Stress Pathways

Expression levels of specific mRNA transcripts for genes involved in pro- and anti-apoptotic pathways were analyzed in primary GCs treated for 18 hours with X:XO (10 μM:2 mU/mL) in the presence or absence of (+)-PTZ (3 μM). Expression levels of the genes involved in ER stress pathways were examined in RGC-5 cells subjected to X:XO (25 μM:10 mU/mL) for various lengths of time (0.5–24 hours) in the presence or absence of (+)-PTZ (3 μM). Total RNA was isolated from the treated cells (TRIzol Reagent; Invitrogen, Carlsbad, CA) and quantified. RNA (5 μg) was reverse transcribed in 20 μL reverse transcription buffer (50 mM Tris-HCl, 75 mM KCl, and 3 mM $MgCl_2$; pH 8.3) containing 10 mM dithiothreitol (DTT), 0.5 mM dNTPs, 0.5 μg oligo (dT) 12-18, and 200 U reverse transcriptase (200 U/μL Superscript II; Invitrogen). Reverse transcription was performed in a thermocycler (Perkin-Elmer 2700; Applied Biosystems, Inc. [ABI], Foster City, CA). PCR reactions were performed in 25 μL PCR buffer (20 mM Tris-HCl, 100 mM KCl, and 2 mM $MgCl_2$ [pH 8.0]) containing 0.2 mM dNTPs, 0.5 μM each pro- and anti-apoptotic gene-specific primer (Table 2), or 0.5 μM for each ER stress pathway–related gene-specific primer (Table 3). PCR reactions for genes related to pro- and anti-apoptotic pathways were performed at 35 cycles, with a denaturing phase of 1 minute at 94°C, an annealing phase of 1 minute at 60°C, and an extension of 1 minute at 72°C. To analyze the expression of ER stress pathway genes, cDNAs were amplified for 45 cycles in PCR mastermix (Absolute SYBR Green Fluorescein; ABgene, Surrey, UK) and gene-specific primers in a real-time PCR detection system (iCycler; Bio-Rad Laboratories, Hercules, CA). Expression levels were calculated by comparison of C_t values ($^{\Delta\Delta}C_t$).[32] For in vivo studies, retinas were harvested from 8-week-old C57Bl/6-*Ins2*$^{Akita/+}$ (diabetic), wild-type, and *Ins2*$^{Akita/+}$ mice that had been maintained on (+)-PTZ, using a dosage regimen that results in robust neuroprotection.[11] RNA was isolated, and the expression of ER stress-related genes was examined by qRT-PCR with primer pairs (Table 3).

Western Blot Analysis

To detect cleaved caspase-3, cleaved caspase-9, σR1, and BiP (GRP78) expression in X:XO-treated cells, we isolated proteins and subjected them to SDS-PAGE.[10] The nitrocellulose membranes to which the proteins had been transferred were incubated with primary antibodies at a concentration of 1:500 (or 1:250 for BiP). They were incubated with HRP-conjugated goat anti-rabbit (Santa Cruz Corp., Santa Cruz, CA) or goat anti-mouse IgG antibody (1:2000; Sigma-Aldrich Corp.). The proteins were visualized with chemiluminescence (SuperSignal West Pico Chemiluminescent Substrate detection system; Pierce Biotechnology, Rockford, IL).

Table 1. Weights and Blood Glucose Levels of *Ins2*$^{Akita/+}$ and Wild-Type Mice

Mouse Group	(+)-PTZ Treatment	*n*	Mean Weight ± SEM (g)	Blood Glucose ± SEM (mg/dL)	Age of Mice/Duration of Diabetes (wk)
Wild-type	No treatment	4	24.7 ± 0.2	242.3 ± 32.6	8 wk/nondiabetic
Wild-type	0.5 mg kg^{-1} 2X/wk ip	4	21.74 ± 1	175.0 ± 5.2	8 wk/nondiabetic
Ins2$^{Akita/+}$	No treatment	6	23.2 ± 0.7	561.8 ± 24.3	8 wk/4 wk diabetic
Ins2$^{Akita/+}$	0.5 mg kg^{-1} 2×/wk ip	5	21 ± 0.3	568.0 ± 22.7	8 wk/4 wk diabetic

TABLE 2. Sequences of Primers for Pro- and Anti-apoptotic Genes

Gene	NCBI Accession No.	Primer Sequence	Predicted Size (bp)
p85	NM_001024955	Forward: 5′-CACGGCGATTACACTCTTACACT-3′ Reverse: 5′-GATGAGGTCCGGCTTAATACTGT-3′	621
p53	NM011640	Forward: 5′-CGCGCCATGGCCATCTAC-3′ Reverse: 5′-AGCTCCCGGAACATCTCGAAG-3′	560
Bcl-2	NM_009741	Forward: 5′-AAGCCGGGAGAACAGGGTATGAT-3′ Reverse: 5′-TGCAGATGCCGGTTCAGGTACTCA-3′	541
p21	NM_007669	Forward: 5′-CGGTGGAACTTTGACTTCGT-3′ Reverse: 5′-CACAGAGTGAGGGCTAAGGC-3′	421
Bcl-xL	U51278	Forward: 5′-TTGGACAATGGACTGGTTGA-3′ Reverse: 5′-ACCCCAGTTTACTCCATCCC-3′	453
c-*myc*	NM_010849	Forward: 5′-CCATCCTATGTTGCGGTCGCT-3′ Reverse: 5′-CTGGTGGTGGGCGGTGTC-3′	533
TRAIL	NM_009425	Forward: 5′-TGGTGATTTGCATAGTGCTCC-3′ Reverse: 5′-TCCTAAAGAGCACGTGGTTGA-3′	468
FasL	BC052866	Forward: 5′-CAGCAGCCCATGAATTACCCATGT-3′ Reverse: 5′-AGTTTCGTTGATCACAAGGCCACC-3′	549
TNF-R	NM_011609	Forward: 5′-TGGCTGTAAGGAGAACCAGTTCCA-3′ Reverse: 5′-TCCACCACAGCATACAGAATCGCA-3′	717
Survivin	AF077349	Forward: 5′-TCTGGCAGCTGTACCTCAAGAACT-3′ Reverse: 5′-AGCTGCTCAATTGACTGACGGGTA-3′	378

Immunocytochemical Detection of Nitrotyrosine in RGC-5 Cells

RGC-5 cells were incubated with X:XO (25 μM:10 mU/mL) in the presence or absence of (+)-PTZ (3 μM) and were subjected to immunocytochemistry to detect nitrotyrosine (1:100; Cell Signaling Technology, Beverly, MA). Nitrotyrosine was detected with goat anti-rabbit IgG conjugated to Cy-3 (Abcam Corp., Cambridge, MA), and the cells were examined by epifluorescence microscopy (Axioplan-2 microscope, equipped with the Axiovision program and HRM camera; Carl Zeiss Meditec). Negative control experiments omitted the primary antibody. The RGC-5 cells were analyzed for the presence of σR1 in co-localization immunocytochemical studies with the ER marker PDI, according to our method.[17]

Cell Viability Assay

Cell viability was measured using the neutral red assay.[33] RGC-5 cells were treated with X:XO (25 μM:10 mU/mL) in the presence or absence of (+)-PTZ (3 μM) for 3, 6, and 18 hours. Neutral red solution (Sigma-Aldrich Chemical Corp.) was added to a final concentration of 0.033% to the cell culture media, the cells were incubated for 2 hours at 37°C, washed with HEPES buffer (125 mM NaCl, 5 mM KCl, 1.8 mM $CaCl_2$, 2 mM $MgCl_2$, 0.5 mM NaH_2Po_2, 5 mM $NaHCO_3$, 10 mM D-glucose, and 10 mM HEPES; pH 7.2). The cells were treated with ice-cold solubilization buffer (ethanol: acetic acid; 5:1; 300 μL/well), and optical densities of samples were read at 570 nm.

Immunoprecipitation Analysis

RGC-5 cells were incubated with X:XO (25 μM:10 mU/mL) in the presence or absence of (+)-PTZ (3 μM) for 3, 6, and 18 hours. After the medium was aspirated, the cells were incubated in 800 μL immunoprecipitation (IP) buffer (1% Triton X-100, 150 mM NaCl, 10 mM Tris pH 7.4, 1 mM EDTA, 1 mM EGTA [pH 8.0], 0.2 mM sodium orthovanadate, 0.5% IGEPAL, and protease inhibitor cocktail) on ice for 10 minutes. Lysates were centrifuged at 14,000*g* for 15 minutes. Protein content of the supernatant was assayed, and 1 mg protein was used for immunoprecipitation. After a 3-hour incubation at 4°C with rabbit

TABLE 3. Sequences of Primers for ER Stress Genes

Gene	NCBI Accession No.	Primer Sequence	Predicted Size (bp)
18S	NR_003278	Forward: 5′-AGTGCGGGTCATAAGCTTGC-3′ Reverse: 5′-GGGCCTCACTAAACCATCCA-3′	90
σR1	NM_030996	Forward: 5′-CATTCGGGACGATACTGGGC-3′ Reverse: 5′-CCTGGGTAGAAGACCTCACTTTT-3′	101
IP3R3	NM_080553	Forward: 5′-AGACCCGCTGGCCTACTATGAGAA-3′ Reverse: 5′-GTCAGGAACTGGCAGATGGCAGGT-3′	111
BiP	NM_022310	Forward: 5′-ACTTGGGGACCACCTATTCCT-3′ Reverse: 5′-ATCGCCAATCAGACGCTCC-3′	134
PERK	NM_010121	Forward: 5′-AGTCCCTGCTCGAATCTTCCT-3′ Reverse: 5′-TCCCAAGGCAGAACAGATATACC-3′	125
ATF4	NM_009716	Forward: 5′-TCCTGAACAGCGAAGTGTTG-3′ Reverse: 5′-ACCCATGAGGTTTCAAGTGC-3′	129
IRE1a	NM_023913	Forward: 5′-ACACCGACCACCGTATCTCA-3′ Reverse: 5′-CTCAGGATAATGGTAGCCATGTC-3′	110
ATF6	NM_001107196	Forward: 5′-TGCCTTGGGAGTCAGACCTAT-3′ Reverse: 5′-GCTGAGTTGAAGAACACGAGTC-3′	141
CHOP	NM_007837	Forward: 5′-CTGGAAGCCTGGTATGAGGAT-3′ Reverse: 5′-CAGGGTCAAGAGTAGTGAAGGT-3′	121

anti-σR1 antibody (1: 25),[34] protein A/G agarose beads (Santa Cruz Corp.) were added and incubated overnight at 4°C. After washing in IP buffer, the immunoprecipitated proteins were denatured at 95°C for 5 minutes in 2× SDS sample loading buffer and 25 μL of total protein was subjected to 10% SDS–PAGE gel and evaluated by Western blot analysis with a mouse monoclonal antibody to phosphoserine (1:500), phosphotyrosine (1:500), or BiP (1:250). Monoclonal antibodies to β-actin, phosphoserine, and phosphotyrosine were from Sigma-Aldrich; mouse BiP monoclonal antibody was from BD Biosciences (Mississauga, ON). After incubation with HRP-conjugated goat anti-mouse IgG antibody, the proteins were visualized by chemiluminescence (SuperSignal West Pico Chemiluminescent Substrate detection system; Pierce Biotechnology).

Microarray Gene Analysis

RNA was isolated from neural retinas of *Ins2*$^{Akita/+}$ mice, *Ins2*$^{Akita/+}$ mice treated with (+)-PTZ, and wild-type mice (age 8 weeks). Total RNA was used to synthesize cDNA probes (FairPlay Microarray labeling kit; Stratagene, La Jolla, CA); probes were labeled with Cy3 or Cy5 monofunctional reactive dye (Amersham Bioscience, Piscataway, NJ). Hybridization of cDNA to mouse gene microarray slides (Mouse One-Array Genome; Phalanx Biotech, Palo Alto, CA,) was performed in triplicate at 43°C for 16 hours. For fluorescence imaging, we used a commercial scanner and software (Genepix 4000B scanner and Genepix pro 4.1 software; Axon Instruments, Union City, CA). The Cy3/Cy5 intensity ratios were normalized and subsequently analyzed (JMP software; SAS Institute, Cary, NC) to compare gene expression profiles quantitatively.

Statistical Analysis

Data were analyzed by one-way analysis of variance (ANOVA; NCSS 2007 statistical package; NCSS Statistical Software Corp., Kaysville, UT). The Tukey-Kramer HSD (honest significant difference) was the post hoc test. $P < 0.05$ was considered significant.

Results

Oxidative stress underlies many retinal degenerative diseases including diabetic retinopathy.[35,36] Primary GCs were exposed to X:XO, which raises extracellular H_2O_2 levels and has been used to simulate oxidative stress in GCs[37]; xanthine oxidase levels increase in diabetes.[38] The primary GCs typically projected numerous neurites from their soma and developed intricate neurite networks, as shown by DIC microscopy (Fig. 1A). The cells incubated with X:XO had limited neuronal processes compared with the controls (Fig. 1B). When X:XO-exposed cells were treated with (+)-PTZ, neurite projections were preserved (Fig. 1C). Treatment with (+)-PTZ alone did not alter neurite projections compared with the control (Fig. 1D). There were significantly more TUNEL-positive cells after X:XO exposure compared to the untreated or oxidatively stressed cultures treated with (+)-PTZ (Figs. 1E–H, Table 4). The findings were confirmed by Western blot, in which cleaved caspase-9 (initiates apoptosis) and cleaved caspase-3 (executes apoptosis) were increased in X:XO-treated cells (Fig. 2A). When the cells were treated with (+)-PTZ, levels of cleaved-caspase-9 and -3 were comparable to control levels. (The slight increase in cleaved caspase-9 in cells treated with (+)-PTZ alone reflects an increase in the total loading of protein in the lane. The β-actin loading control was slightly greater in that condition; however, the densitometric ratio was equivalent to the control and X:XO-treated conditions). We examined the levels of several pro- and anti-apoptotic genes (Figs. 2B. 2C) and found that X:XO-treated cells increased expression of FasL and TRAIL, which was reversed with (+)-PTZ treatment (Fig. 2B). Survivin, a member of the inhibitory of apoptosis (IAP) gene family, was increased markedly in the X:XO-incubated

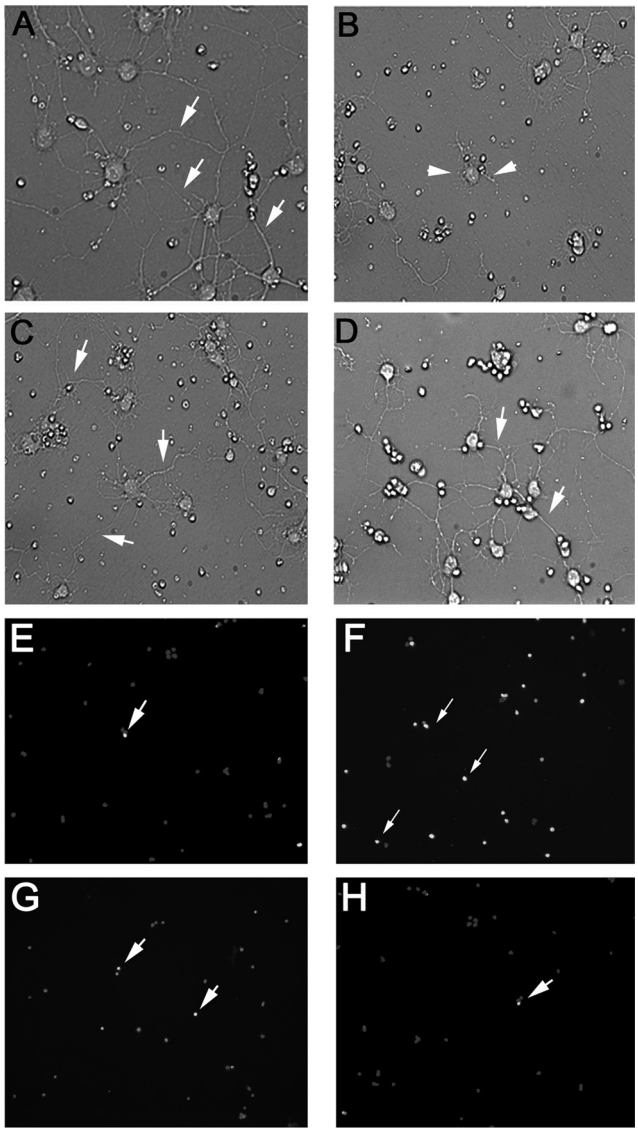

Figure 1. (+)-PTZ prevents oxidative stress-induced apoptotic death of GCs. Primary GCs were subjected to oxidative stress for 18 hours using X:XO at a concentration ratio of 10 μM:2 mU/mL in the presence or absence of (+)-PTZ (3 μM) and were analyzed by DIC microscopy to demonstrate neurite processes (*arrows*). (**A**) No treatment, (**B**) X:XO-exposed cells, (**C**) X:XO-exposed cells treated with (+)-PTZ, and (**D**) cells treated with (+)-PTZ alone. Companion experiments were performed to detect dying cells indicated by a positive reaction (*white*) in the TUNEL assay. *Gray*: nuclei of cells counterstained with Hoechst 33342. (**E**) No treatment, (**F**) X:XO-exposed cells, (**G**) X:XO-exposed cells treated with (+)-PTZ, and (**H**) cells treated with (+)-PTZ alone. Quantitative details for this experiment are provided in Table 4.

cells co-treated with (+)-PTZ (Fig. 2C). The expression level of σR1 was compared between control primary GCs and primary GCs exposed to oxidative stress (X:XO; 10 μM:2 mU/mL, 3, 6, or 18 hours) in the presence or absence of (+)-PTZ (3 μM). Protein was extracted, and σR1 was analyzed by immunoblot analysis. σR1 levels did not differ between the control and oxidatively stressed cells, whether treated with (+)-PTZ or not (data not shown). To determine whether the effects of (+)-PTZ were due to a direct chemical interaction with X:XO, we used a xanthine oxidase assay (BioVision) to calculate the level of H_2O_2 generated when xanthine oxidase oxidized xanthine in the presence or absence of (+)-PTZ. We determined that X:XO (25 μM:10mU/mL) produced 2.23 ± 0.24 and 2.27 ± 0.26

TABLE 4. Quantitation of TUNEL-Positive Primary GCs after X:XO Treatment in the Presence/Absence of (+)-PTZ

Treatment	Number of Fields Analyzed	Number of Cells/Field Range (Mean ± SE)	TUNEL-Positive Cells/Field Range (Mean ± SE)	Percentage TUNEL-Positive Cells: Total Number of Cells/Field
Control	35	13–80 (32.4 ± 2.8)	0–10 (1.7 ± 0.4)	7.0 ± 1.9
X:XO	43	23–149 (54.2 ± 4.9)	2–59 (15.1 ± 2.1)*	30.1 ± 3.0*
X:XO-(+)-PTZ	32	24–98 (42.4 ± 3.5)	0–29 (4.7 ± 1.2)	12.3 ± 3.3
(+) PTZ	35	17–138 (55.8 ± 5.5)	0–12 (2.4 ± 0.5)	5.1 ± 1.5

* Significantly different from (+)-PTZ-treated and control; $P < 0.01$.

mU/mL of H_2O_2 in the absence or presence of (+)-PTZ, respectively; and that X:XO (10 μM:2 mU/mL) produced 0.18 ± 0.06 and 0.17 ± 0.02 mU/mL of H_2O_2 in the absence/presence of (+)-PTZ, respectively. Thus, it appears that the effects of (+)-PTZ are not due to direct chemical interaction with X:XO.

Analysis of the σR1 interaction with BiP (σR1–BiP binding) necessitated immunoprecipitation techniques, which require a large number of cells, thus precluding the use of primary GCs. RGC-5 cells, a mouse neuronal precursor line reported as suitable for analysis of oxidative stress,[39] were used for these studies. σR1 was detected in the perinuclear region and colocalized with PDI (ER-marker; Figs. 3A–D) indicating that RGC-5 cells express σR1 on the ER membrane. RGC-5 cells cultured in the presence of X:XO (25 μM:10 mU/mL) were used to detect nitrotyrosine, a marker of cellular stress (Fig. 3F). Levels of nitrotyrosine diminished to control levels when oxidatively stressed RGC-5 cells were treated with (+)-PTZ (Fig. 3G). Results of the neutral red cell viability assay (Sigma-Aldrich Corp.) showed that short (3- and 6-hour) treatment of RGC-5 cells with X:XO did not affect viability significantly; however, 18-hour exposure to X:XO (25 μM:10 mU/mL) decreased viability by ~20% to 30%. Viability improved significantly in the presence of (+)-PTZ (Fig. 3H).

Cell death ensues after ER stress when adaptive mechanisms (restoration of homeostasis) fail.[40] The role of σR1 as a Ca^{2+}-sensitive, ligand-mediated receptor chaperone at the mitochondrion-associated ER membrane, coupled with reports that σR1 forms a complex with the molecular chaperone BiP,[15] prompted us to examine the interaction between σR1 and BiP. RGC-5 cells were treated with X:XO (25 μM:10 mU/mL) in the presence or absence of 3 μM (+)-PTZ for 3, 6, and 18 hours. σR1 (27 kDa) was detected by Western blot (Fig. 4A), and levels of this protein were equivalent (regardless of X:XO or (+)-PTZ treatment; Fig. 4A). σR1–BiP binding was investigated by immunoprecipitation analysis using antibody against σR1. The immunoprecipitates were used for immunoblot analysis with antibodies specific for BiP/GRP78 (Fig. 4A). We observed marked interaction between σR1 and BiP when the cells were exposed to oxidative stress, whereas such interaction was not evident when they were treated with (+)-PTZ (Fig. 4C). The data suggest that σR1 interacts with BiP in retinal neuronal cells in oxidative stress conditions.

σR1 contains several serine and tyrosine residues. Two of the serines have consensus sequences required for phosphorylation: Ser-117 and Ser-192; there are no consensus sequences for phosphorylation of tyrosine (determined using NetPhos 2.0 software, http://www.cbs.dtu.dk/services/NetPhos/ provided in the public domain by the Center for Biological Sequence Analysis [CBS], Department of Systems Biology, Technical University, Lyngby, Denmark). We investigated whether there was any difference in σR1 phosphorylation under oxidative stress conditions by analyzing the immunoprecipitates, obtained with σR1 antibody by Western blot, using antibodies specific for phosphoserine or phosphotyrosine. We observed a robust increase in phosphorylation of serine in σR1 in oxidative stress conditions (Fig. 4D). When oxidatively stressed cells were treated with (+)-PTZ, phosphorylation of serine in σR1 was minimal. These data suggest that phosphorylation of σR1 is obligatory for its interaction with BiP. As predicted, phosphorylation of tyrosine was not detected in σR1.

The finding that oxidative stress altered σR1 binding to BiP led us to investigate the expression of transmembrane ER proteins regulated by BiP, including PERK, IRE1, ATF6. RGC-5 cells were exposed to X:XO (25 μM:10 mU/mL) in the presence or absence of 3 μM (+)-PTZ for 0, 1, 2, 4, 6, 8, 12, 18, and 24 hours. RNA was isolated (Trizol; Invitrogen); primer pairs specific for BiP, PERK, ATF6, IRE1, ATF4, and CHOP were designed; and RT-qPCR was performed. The ratio of change in gene expression in cells exposed to X:XO in the presence or absence of (+)-PTZ was quantified. Data are presented relative to control (non-X:XO exposed cells assigned an arbitrary value of 1). The data show that exposure to X:XO upregulated expression of BiP (~12–14-fold), the ER stress genes PERK (~4-fold), ATF6 (~2–5 fold), and IRE1 (~4-fold), as well as downstream genes ATF4 (~4-fold) and CHOP (4–9-fold; Fig. 5). There was a marked effect of (+)-PTZ treatment on the expression of these ER stress genes. Exposure

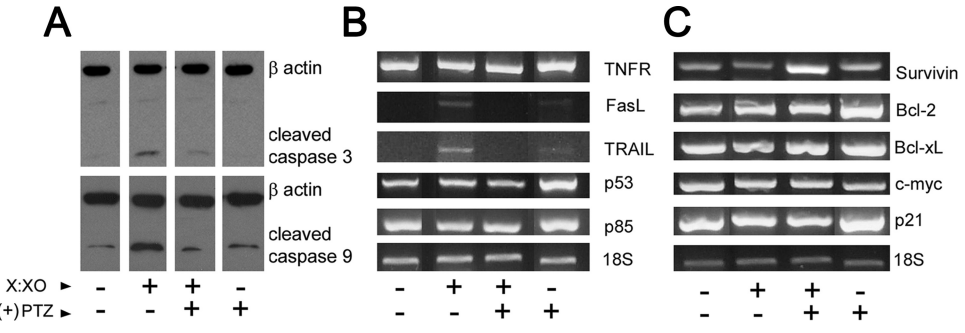

FIGURE 2. Effects of (+)-PTZ on pro- and anti-apoptotic protein and gene expression. Primary GCs were subjected to oxidative stress for 18 hours using X:XO at a concentration ratio of 10 μM:2 mU/mL in the presence or absence of (+)-PTZ (3 μM). (**A**) Western blot assessment of cleaved caspase-3 and -9 in primary retinal GCs subjected to oxidative stress in the absence or presence of (+)-PTZ. Companion experiments were performed in which total RNA was isolated and used for semiquantitative RT-PCR analysis of proapoptotic (**B**) and antiapoptotic (**C**) genes using primer pairs specific for mouse (Table 2). 18S RNA (315 bp) was analyzed in the same RNA samples as an internal control. Data are representative of results in at least two experiments.

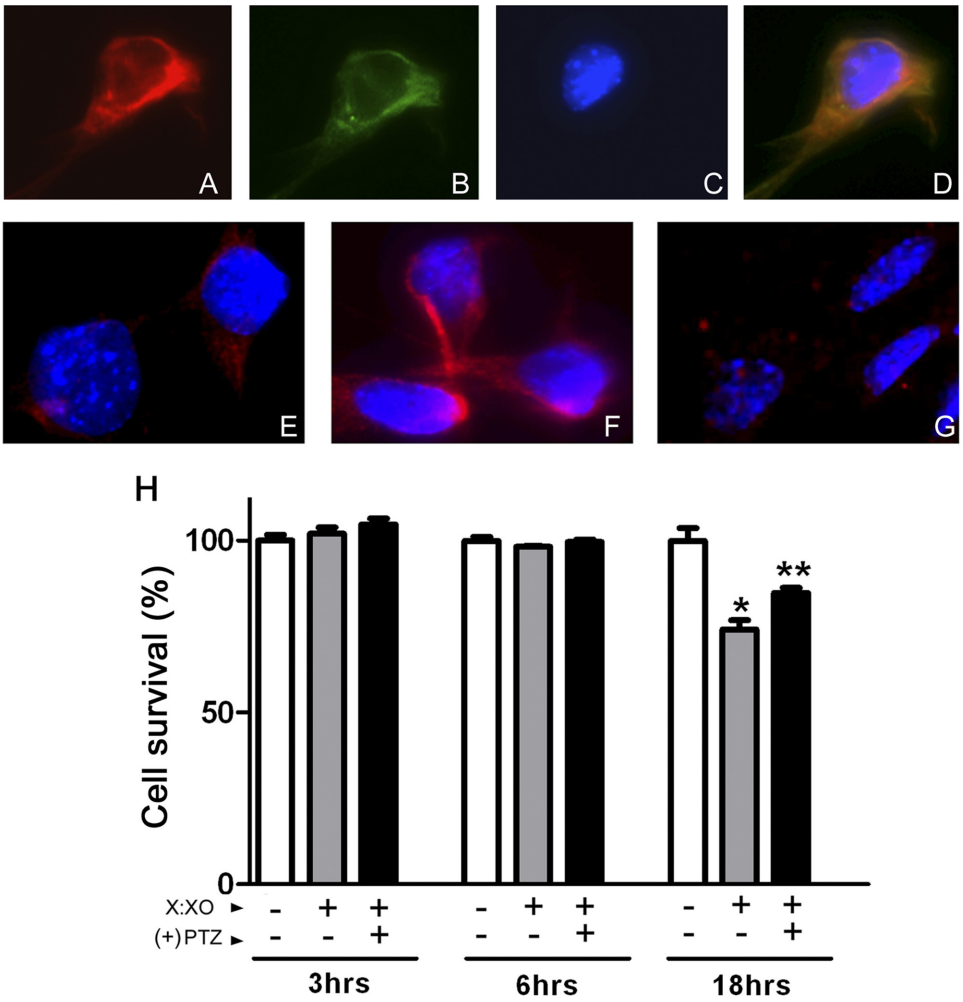

FIGURE 3. Immunocytochemical detection of σR1 and nitrotyrosine in RGC-5 cells. The cells were subjected to immunocytochemical analysis to detect σR1 (**A**, *red* fluorescence) and PDI, an ER marker protein (**B**, *green* fluorescence). DAPI was used to stain the nucleus (**C**) and the merged image shows co-localization of σR1 with PDI (**D**, *orange-yellow* fluorescence). Nitrotyrosine was detected by incubating RGC-5 cells in the absence (**E**) or presence (**F**) of X:XO (25 μM:10 mU/mL) for 18 hours or (**G**) X:XO (25 μM:10 mU/mL) plus (+)-PTZ (3 μM) for 18 hours. The cells were immunolabeled with anti-nitrotyrosine; a positive reaction appears as bright *red* fluorescence (**F**) indicative of increased cellular stress. (**H**) The neutral red assay was performed to assess cell viability after exposure to X:XO (25 μM:10 mU/mL) in the presence or absence of (+)-PTZ (3 μM) for 3, 6, and 18 hours. *Significantly different from control ($P < 0.05$); **significantly different from X:XO-treated cells ($P < 0.05$). Data were performed two times in triplicate.

of cells to X:XO in the presence of (+)-PTZ attenuated their upregulation; gene expression levels were similar to the control. Taken collectively, these data suggest that oxidative stress increases expression of ER stress genes, which is reversed by (+)-PTZ. We examined the expression of σR1 under X:XO stress and observed a transient upregulation at 1 hour followed by a slight decrease in expression over the 24-hour X:XO exposure period. (+)-PTZ treatment maintained σR1 expression at normal levels. In these experiments, we evaluated expression of the gene encoding IP_3R_3 (inositol 1,4,5-triphosphate receptor type 3), since IP_3Rs govern the release of Ca^{2+} stored within the ER lumen[41] and σR1 stabilizes IP_3Rs at the mitochondrial-associated ER membrane.[15] As we observed with σR1, there was no significant difference in IP_3R_3 mRNA over the period studied for X:XO cells in the presence or absence of (+)-PTZ. The data show a transient increase (first 2 hours) in IP_3R_3 and then a slight decrease over the next 20 hours of X:XO exposure (Fig. 5). Overall, expression of IP_3R_3 did not differ between X:XO exposure regardless of the (+)-PTZ treatment.

To determine whether these in vitro findings were relevant to (+)-PTZ effects in vivo, we examined the expression of ER stress genes in the *Ins2*$^{Akita/+}$ mouse model of diabetic retinopathy in which one group of mice received (+)-PTZ treatment. This model was examined because the diabetic mice demonstrate ~20% to 25% reduction of retinal inner plexiform layer thickness, ~16% reduction of inner nuclear layer thickness and ~25% reduction in the number of cell bodies in the GC layer.[11,25,26] (+)-PTZ conferred profound preservation of retinal phenotype in this model when (+)-PTZ was administered to mice at the onset of diabetes.[11] In the current work, *Ins2*$^{Akita/+}$ mice were treated at diabetes onset (3–4 weeks), with or without (+)-PTZ (0.5 mg kg^{-1}) twice weekly for 4 weeks, at which time RNA was isolated from neural retinas and subjected to RT-qPCR to evaluate expression of BiP, PERK, ATF6, IRE1, ATF4, CHOP, and IP_3R_3. The expression of ER stress genes in these mice was compared to age-matched wild-type mice for which mRNA levels for ER stress genes were assigned an arbitrary value of 1. As shown in Figure 6, the expression of several ER stress genes increased in neural retinas of diabetic mice. For example, BiP expression increased compared with that in the wild-type mice, as did PERK, ATF6, IRE1, ATF4, and CHOP. The retinas of *Ins2*$^{Akita/+}$ mice treated with (+)-PTZ showed a decreased expression of most of these genes, in some cases to a level very similar to that in the age-matched controls (PERK, ATF6, IREI, and ATF4). IP_3R_3 levels increased in the retinas of *Ins2*$^{Akita/+}$ mice and decreased when *Ins2*$^{Akita/+}$ mice were treated with (+)-PTZ.

We examined the retinal transcriptome of *Ins2*$^{Akita/+}$ mice to determine other more broadly expressed genes that were altered in the diabetic retina, but reversed after (+)-PTZ treatment. Retinal RNA was isolated from *Ins2*$^{Akita/+}$ mice that were 8 weeks (age-matched diabetic mice with or without (+)-PTZ treatment as well as age-matched, nondiabetic wild-type mice). The DNA microarray slide used allows for evaluation of 29,992 genes. There were approximately 900 genes with expression that was altered (either up- or downregulated)

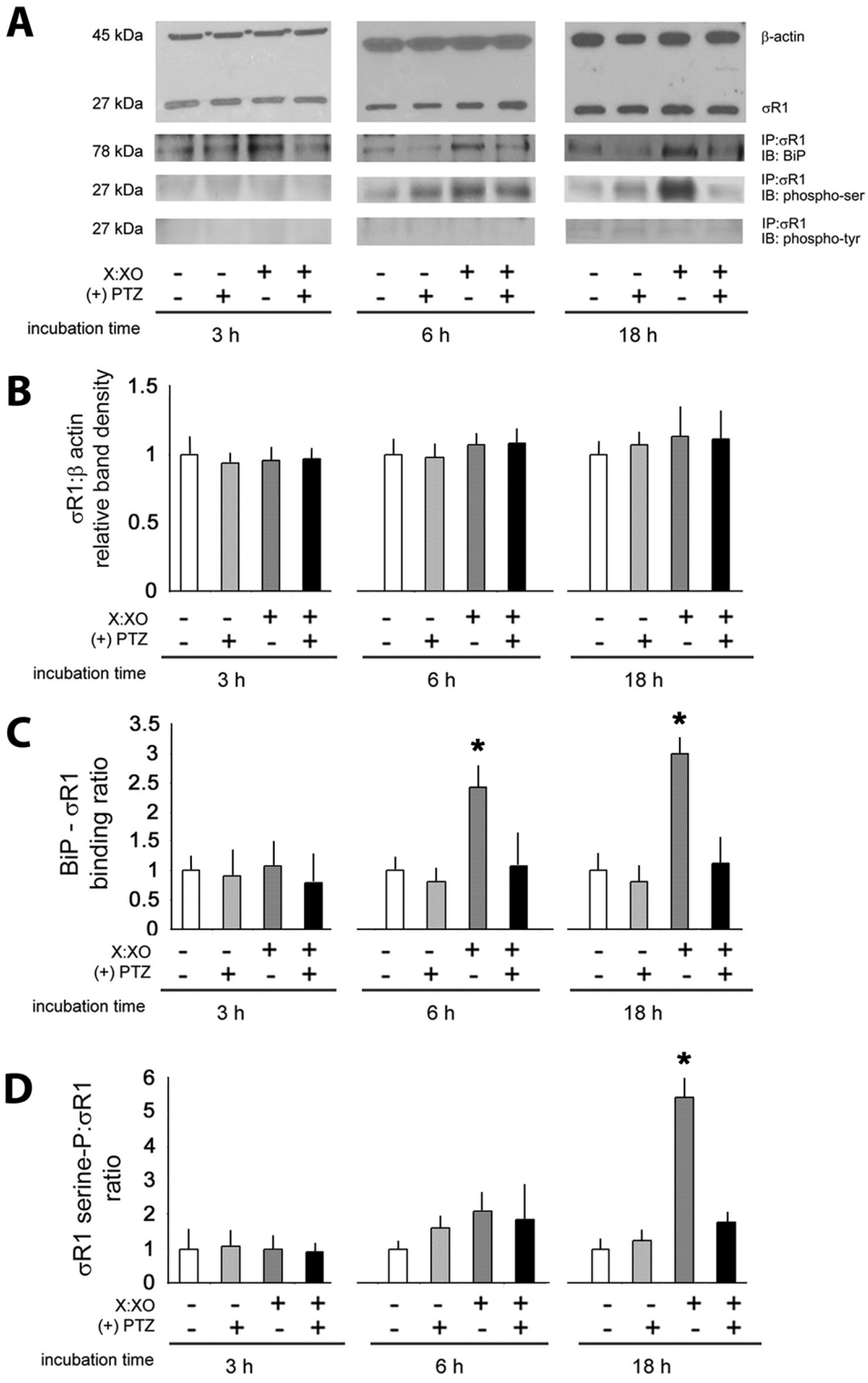

FIGURE 4. Analysis of σR1–BiP interaction and σR1 phosphorylation. RGC-5 cells were treated with X:XO (25 μM:10 mU/mL) in the presence or absence of 3 μM (+)-PTZ for 3, 6, and 18 hours. (**A**) Total protein was isolated and σR1 (27 kDa) detected by immunoblot analysis in RGC-5 cells. β-Actin (45 kDa) served as the internal standard. Immunoprecipitation was performed with σR1 antibody, and the immunoprecipitates were then subjected to Western blot to detect BiP, phosphoserine, and phosphotyrosine. Bar graphs show the densitometric quantification of σR1:β actin (**B**), σR1:BiP binding normalized to β-actin (**C**) or σR1: phosphoserine normalized to β actin (**D**). The relative ratio in control cells (cells not exposed to X:XO or (+)-PTZ) was assigned the arbitrary value of 1. Data are the mean and SEM from two or three independent experiments. *Significantly different from the control ($P < 0.05$).

by a log factor greater than 1.7 in the comparison of *Ins2*$^{Akita/+}$ with wild-type mice and *Ins2*$^{Akita/+}$ versus (+)-PTZ-treated *Ins2*$^{Akita/+}$ mice. Table 5 shows 23 genes with expression that was altered in *Ins2*$^{Akita/+}$ mice (compared with wild-type) and was then reversed when *Ins2*$^{Akita/+}$ mice were treated with (+)-PTZ. Genes that were altered included those whose protein products are involved in apoptosis, axon guidance, calcium ion binding, and cell differentiation. A complete list of genes altered by a factor greater than 2 is provided in Tables 6 and 7.

DISCUSSION

This study explored mechanisms by which (+)-PTZ, a ligand for σR1, mediates retinal neuroprotection. Retinal neurons, including GCs, die in sight-threatening diseases such as diabetic retinopathy; oxidative stress is implicated in this death. Previously, we reported that the excitotoxin-induced death of primary mouse GCs and retinal neuronal (RGC-5) cells was attenuated markedly when the cells were incubated with (+)-PTZ.[1,2] Subsequent in vivo

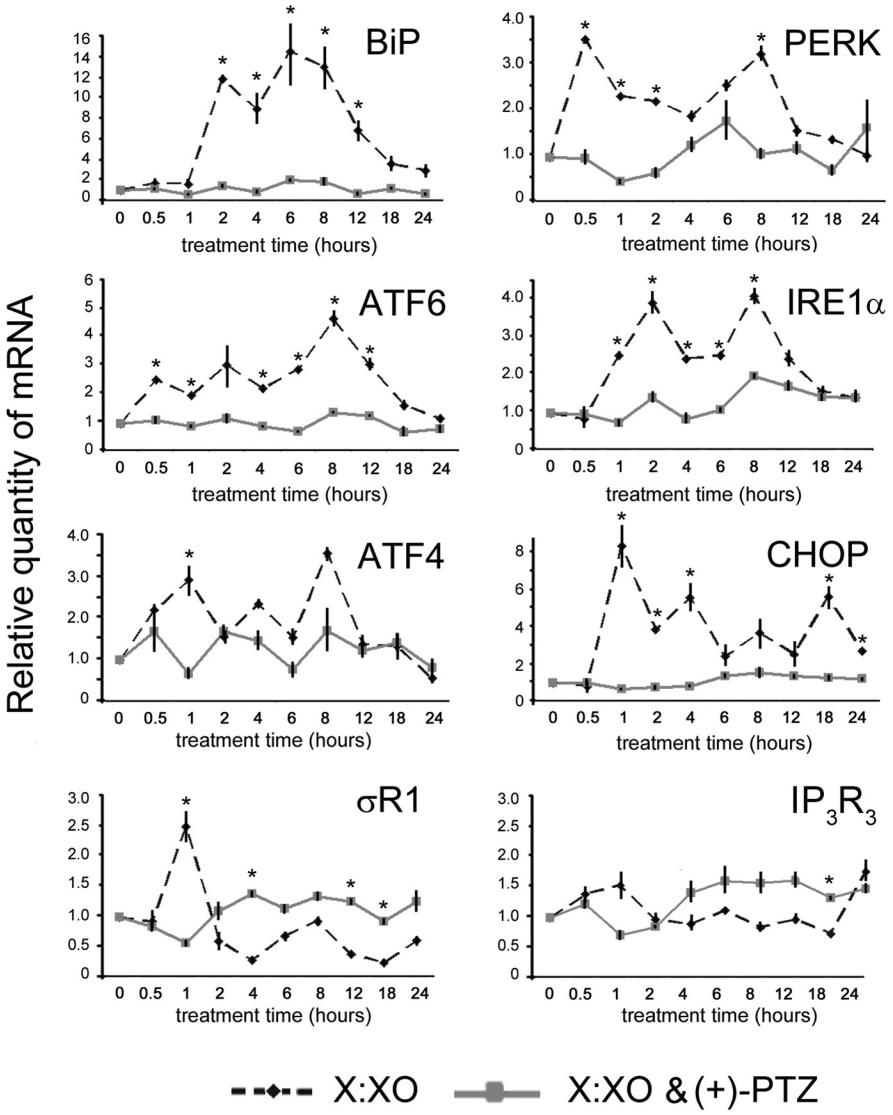

FIGURE 5. qRT-PCR analysis of ER stress genes in vitro. RGC-5 cells were treated with X:XO (25 μM:10 mU/mL) in the presence or absence of 3 μM (+)-PTZ over a 24-hour period, and the expression of the ER stress genes was analyzed by qRT-PCR with the primers listed in Table 3. *Significantly different gene expression in X:XO-exposed cells in the absence versus the presence of (+)-PTZ ($P < 0.05$). Data represent the mean ± SEM of three experiments.

experiments examined the effects of (+)-PTZ in diabetic *Ins2*$^{Akita/+}$ mice, because its noticeable loss of RGCs and alterations of various cellular layers[11,25,26] are reversed when mice are maintained on (+)-PTZ over the course of many weeks.[11]

In the present study, we investigated the mechanism of σR1 neuroprotection in retinal neurons in vitro and in vivo. Recent data suggest that σR1 functions as a molecular chaperone at the ER–mitochondrion interface that regulates cell survival. σR1 forms a complex with another molecular chaperone, BiP.[15] In CHO cells, acute injury (glucose deprivation or tunicamycin treatment) led to a rapid, transient increase in σR1 levels (a marked increase within 1 to 3 hours with a return to baseline, or lower, by 6 hours). No change in BiP levels was observed. The same model system was used to examine how exposure of cells to the ER stressor, thapsigargin (Ca^{2+}-ATPase inhibitor) or glucose deprivation, altered σR1–BiP binding. σR1 dissociated from BiP within 5 minutes of exposure to thapsigargin, and the dissociated state persisted for the 60-minute duration of the experiment.[15] In the glucose deprivation paradigm, however, there was a transient increase in σR1–BiP binding over 30 minutes with dissociation observed by 60 minutes. Thus, it appears that depending on the nature of the stressor, the binding of σR1–BiP varies. This seminal work showed that (+)-PTZ treatment dissociates σR1 from BiP, suggesting that σR1 agonists exert their effects by freeing σR1 from BiP.

These important observations laid the foundation of the present study investigating how chronic in vitro (oxidative stress model) and in vivo stress (diabetes) affect σR1 and BiP expression in retinal neurons, how the interaction between these proteins may be altered during oxidative stress, and whether (+)-PTZ alters σR1–BiP binding and expression of ER stress-related genes in these models. Oxidative stress was examined because it is implicated in the pathophysiology of neuronal death in diabetic retinopathy,[35,36] and our previous studies showed marked rescue by (+)-PTZ of neuronal death in an in vivo diabetic model.[11] In the current work, our experiments conducted in primary GCs revealed marked sensitivity to oxidative stress, characterized by neurite process disruption and cellular apoptosis. Oxidative stress increased expression of the proteins that initiate and execute apoptosis (caspase-9 and -3, respectively) and the upstream pro-apoptotic genes *FasL* and *TRAIL*. (+)-PTZ reduced caspase-9 and -3 levels and the pro-apoptotic genes. Expression of the anti-apoptotic gene survivin increased when oxidatively stressed cells were treated with (+)-PTZ. Neurite disruption detected in primary GCs exposed to oxidative stress was not observed in cells treated with (+)-PTZ.

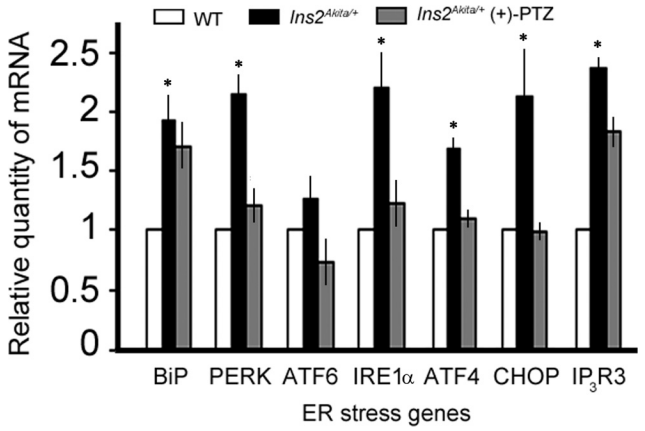

FIGURE 6. qRT-PCR analysis of ER stress genes in vivo. Total RNA was isolated from neural retinas of wild-type and C57Bl/6-*Ins2*$^{Akita/+}$ mice (age: 8 weeks, 4 weeks diabetic, $n = 6$ per group), which had been maintained in the absence or presence of 0.5 mg kg^{-1} (+)-PTZ (intraperitoneal injection twice a week for 4 weeks). The expression of ER stress genes was analyzed by qRT-PCR using the primers listed in Table 3. *Significantly different from wild-type retina ($P < 0.05$). Data represent the mean ± SEM of analyses of three sets of tissues per group.

These findings are relevant to the report of σR1-induced potentiation of growth factor-stimulated neurite outgrowth in neuronal cell lines (PC12).[41]

To analyze the interaction of σR1 with BiP under oxidative stress required the use of the retinal RGC-5 neuronal cell line. Exposing these cells to oxidative stress did not alter σR1 protein levels over the 18-hour period examined; however it did alter the binding of σR1 to BiP, such that σR1–BiP binding increased with oxidative stress. When the cells were treated with (+)-PTZ (3 μM), σR1–BiP binding was at baseline level. Our data are similar to those in the glucose-deprivation model reported earlier,[15] wherein the σR1–BiP interaction appeared to increase rather than the thapsigargin stress model in which σR1 dissociated from BiP.

Many proteins are regulated by phosphorylation resulting in an increase or decrease of biological activity, movement between subcellular compartments, and interactions with other proteins. We asked whether there are differences in σR1 phosphorylation under oxidative stress conditions, specifically phosphorylation of serine and tyrosine residues. While there was no difference in tyrosine phosphorylation under stress, but there was a robust increase in phosphorylation of serine (sixfold by 18 hours of oxidative stress). σR1 serine phosphorylation in oxidatively stressed cells decreased markedly when the cells were treated with (+)-PTZ. This report is the first to identify σR1 as a phosphoprotein. Our studies show that phosphorylation of the receptor is altered by cellular stress and by exposure to the receptor ligands. Phosphorylation of σR1 may facilitate its binding to BiP, as the increase in σR1–BiP interaction parallels phosphorylation of σR1. Additional studies are

TABLE 5. Gene Expression Data for Retinas of *Ins2*$^{Akita/+}$ Diabetic Mice with or without Treatment with (+)-PTZ

Accession Number	Gene	Gene Function	Change Ratio	
			Akita/WT	(+)-PTZ-Akita/Akita
NM_207653	CASP8 & FADD-like apoptosis regulator (*Cflar*)	Proapoptotic, FAS signaling	+3	−2
NM_019635	Serine/threonine kinase 3 (*STK3*)	Proapoptotic	+1.9	−2
NM_007906	Eukaryotic elongation translation factor 1 (*Eef1a2*)	Antiapoptotic	−3	+2.4
NM_008142	Guanine nucleotide binding protein (*Gnb1*)	Cell proliferation	−2	+2.7
NM_011356	Frizzled related protein (*Frzp*)	Cell differentiation	−6	+7
NM_011664	Ubiquitin B (*UbB*)	Neurodegenerative diseases	+3	−2.7
NM_001113330	Cone-rod homeobox containing gene (*Crx*)	Photoreceptor differentiation	+2	−2.5
NM_007568	Betacellulin, EGF family member (*Btc*)	Abnormal retinal layering	+2	−2.3
NM_010228	VEGF receptor 1	Cell differentiation, proliferation	+2	−2
NM_144761	Crystallin, gamma B (*CrysGB*)	Lens constituent	−4	+9
NM_007776	Crystallin, gamma D (*CrysGD*)	Lens constituent	−5	+10
NM_015748	Slit homolog 1 (drosophila)	Axon guidance/inhibit neurite outgrowth	+5	−6
NM_031255	Radial spokehead-like 1 (*Rshl1*)	Cilium	−2	+2
NM_007887	Deubiquinating enzyme 1 (*Dub1*)	Axon development	−4	+2
NM_031165	Heat shock protein 8 (*HSP8*)	ER stress indicator	+2	−2
NM_011508	Eukaryotic elongation translation factor 1 (Eif1)	Increased in oxidative stress	+1.7	−1.7
NM_023371	Protein (peptidyl prolyl cis/trans isomerase)	Decreased in oxidative stress	+2	−1.8
NM_009118	Retinal S antigen	Calcium ion binding	+3	−2.9
NM_001077510	Guanine nucleotide binding protein (*GNAS*)	Calcium ion binding	−2	+2
NM_010017	Dystroglycan 1 (*Dag1*)	Calcium ion binding	−2	+2.5
NM_023279	Tubulin β-3	Gap junction	−2	+2.1
NM_013592	Matrillin 4	Filamentous networks of ECM	−2	+4.1
NM_194060	Forkhead box 06 (*FOXO6*)	Gene regulation	+2.8	−5

RNA was isolated from the neural retinas of wild-type mice and diabetic *Ins2*$^{Akita/+}$ mice that either had or had not been treated over a period of 4 weeks with (+)-PTZ and subjected to microarray analysis. Information is shown about genes with expression that was altered in the diabetic mouse compared with wild-type (WT) and was reversed when the mice were treated with (+)-PTZ. The first column of change ratios refers to either an increase (positive value, e.g. +3) or decrease (negative value, e.g. −2) in the *Ins2*$^{Akita/+}$ mice compared to WT; the second column provides data for (+)-PTZ-treated *Ins2*$^{Akita/+}$ mice compared with untreated *Ins2*$^{Akita/+}$ mice. (Thus, the expression of the first gene *Cflar,* a proapototic gene, was increased in *Ins2*$^{Akita/+}$ mice by threefold compared with WT and was decreased twofold in (+)-PTZ-treated *Ins2*$^{Akita/+}$ mice compared with untreated *Ins2*$^{Akita/+}$ mice.)

TABLE 6. Retinal Gene Expression Differences in *Ins2*$^{Akita/+}$ Mice Compared with 8-Week-Old Wild-Type Mice

Accession Number	Gene	Function	Change Ratio
Apoptosis			
NM_009805	CASP8 and FADD-like apoptosis regulator (*Cflar*)	FAS signaling pathway	+3
NM_008048	Insulin-like growth factor binding protein 7 (Igfbp7)	Induction apoptosis	+2
NM_028072	Sulfatase 2 (*Sulf2*)	Induction apoptosis	+2
NM_013492	Clusterin (*Clu*)	Induction apoptosis	+2
NM_001025600	Cell adhesion molecule 1 (*Cadm1*)	Induction apoptosis	+2
NM_008410	Integral membrane protein 2B (*Itm2b*)	Induction apoptosis	+1.9
NM_019635	Serine/threonine kinase 3 (Ste20, yeast homolog) (*Stk3*)	Induction apoptosis	+1.9
NM_027318	Zinc finger, HIT domain containing 1 (*Znhit1*)	Induction apoptosis	−3
NM_001128151	Cat eye syndrome chromosome region, Candidate 2 homolog (human) (*Cecr2*)	Induction apoptosis	−5
Antiapoptosis			
NM_011711	Formin-like 3 (*Fmnl3*)	Functions in cell growth and proliferation	+3
NM_007906	Eukaryotic translation elongation factor 1 alpha 2 (*Eef1a2*)	Antiapoptosis	+3
NM_025788	BTB (POZ) domain containing 14B (*Btbd14b*)	Tumorigenesis	+2
NM_008142	Guanine nucleotide binding protein (G protein), beta 1 (*Gnb1*)	Cell proliferation	+2
NM_011356	Frizzled-related protein (*Frzb*)	Cell differentiation	−6
Cell Cycle			
NM_023223	Cell division cycle 20 homolog (*S. Cerevisiae*) (*Cdc20*)	Cell cycle	+2
NM_011299	Ribosomal protein S6 kinase, polypeptide 2 (*Rps6ka2*)	Controlling cell growth and differentiation; MAP kinase signaling pathway	−2
NM_027764	Regulator of chromosome condensation (RCC1) and BTB (POZ) domain containing protein 1 (*Rcbtb1*)	Cell cycle	−4
Neuron/Retina/Eye Development			
NM_013501	Crystallin, alpha A (*Cryaa*)	Camera-type eye development	+4
NM_007773	Crystallin, beta B2 (*Crybb2*)	Structural constituent of eye lens	+3
	Ubiquitin B (*Ubb*)	Neurodegenerative diseases	+3
NM_009964	Crystallin, alpha B (*Cryab*)	Camera-type eye development	+2
NM_021541	Crystallin, beta A2 (*Cryba2*)	Structural constituent of eye lens	+2
NM_007568	Betacellulin, epidermal growth factor Family member (*Btc*)	Over expression showed abnormal retinal layer	+2
NM_001113330	Cone-rod homeobox containing gene (*Crx*)	Differentiation of photoreceptor cell	+2
NM_018780	Secreted frizzled-related sequence protein 5 (*Sfrp5*)	SFRP5 and SFRP1 may be involved in determining the polarity of photoreceptor cells in the retina	+2
NM_010228.3	Ferritin light chain 1 (*Flt1*)	Neurodegenerative	+2
NM_027256	Integrator complex subunit 4 (*Ints4*)	Neuroplasticity, apoptosis, and cytoskeletal regulation	−3
NM_144761	Crystallin, gamma B (*Crygb*)	Eye development; structural constituent of eye lens	−4
NM_133719	Meteorin, glial cell differentiation regulator (*Metrn*)	Glial cell differentiation	−4
NM_007776	Crystallin, gamma D (*Crygd*)	Eye development; structural constituent of eye lens	−5
Axon			
NM_015748	Slit homolog 1 (*Drosophila*) (*Slit1*)	Axon guidance; inhibit neurite outgrowth	+5
NM_031255	Radial spokehead-like 1 (*Rshl1*)	Cilium	−2
NM_007887	Deubiquitinating enzyme 1 (*Dub1*)	Axon budding	−4
Oxidative Stress/ER Stress			
NM_031165	Heat shock protein 8 (*Hspa8*)	ER stress indicator	+2
NM_011508	Eukaryotic translation initiation factor 1 (*Eif1*)	Upregulated under oxidative stress	+1.7
NM_023371	Protein (peptidyl-prolyl cis/trans Isomerase) NIMA-interacting 1 (*Pin1*)	Decreased under ER stress	−1.8
NM_009656	Aldehyde dehydrogenase 2, mitochondrial (*Aldh2*)	Protector from oxidative stress	−2
Calcium Signaling			
NM_009118	Retinal S-antigen (*Sag*)	Calcium ion binding	+2.9
NM_018804	Synaptotagmin XI (*Syt11*)	Calcium ion binding	+2
NM_207650	Dystrobrevin alpha (*Dtna*)	Calcium ion binding	+2
NM_001077510	GNAS (guanine nucleotide binding protein, alpha stimulating) complex locus (*Gnas*)	Calcium signaling pathway	−2

(*continues*)

TABLE 6 (*continued*). Retinal Gene Expression Differences in *Ins2$^{Akita/+}$* Mice Compared with 8-Week-Old Wild-Type Mice

Accession Number	Gene	Function	Change Ratio
NM_010017	Dystroglycan 1 (*Dag1*)	Calcium ion binding	−2.5
ECM Regulation			
NM_001081242	Talin 2 (*Tln2*)	Actin binding	+2.5
NM_011653	Tubulin, alpha 1A (*Tuba1a*)	Gap junction	+2.1
XM_284166	PREDICTED: amelotin (*Amtn*)	Basal lamina	+2.1
NM_008610	Matrix metallopeptidase 2 (*Mmp2*)	Degradation of ECM	+2
NM_001008231	Dishevelled associated activator of morphogenesis 2 (*Daam2*)	Actin binding	−2.1
NM_023279	Tubulin, beta 3 (*Tubb3*)	Gap junction	−2.1
NM_009926	Collagen, type XI, alpha 2 (*Col11a2*)	Cell adhesion	−2.6
NM_013592	Matrilin 4 (*Matn4*)	Formation of filamentous networks in the extracellular matrices	−4.1
Miscellaneous			
NM_007898	Phenylalkylamine Ca2+ antagonist (emopamil) binding protein (*Ebp*)	Similar with sigma receptor 1 and has a drug binding affinity, located at ER	+2
NM_011618	Troponin T1, skeletal, slow (*Tnnt1*)	Upregulated by NMDAR antagonist	−3.6
NM_029376.2	Spermatogenesis associated glutamate (E) rich protein 4a (*Speer4a*)	-	−5.4

needed to demonstrate this potentially interesting and important phenomenon unequivocally. σR1 contains two serine residues that contain consensus sequences for phosphorylation (Ser-117 and Ser-192). Site-directed mutagenesis techniques will be used to analyze comprehensively whether elimination of one or both σR1 phosphorylation sites alters or disrupts the σR1 binding of (+)-PTZ, the σR1 binding to BiP, and/or the ER subcellular localization of σR1.

It is likely that σR1 binding to proteins is not limited to BiP as we (present study) and others[15] have shown. Co-immunoprecipitation studies performed in RGC-5 cells demonstrated an association between L-type calcium channels and σR1,[13] although these investigators did not examine whether there was an alteration in the interaction as a consequence of cellular stress. It is noteworthy that σR1 interacts with other proteins including opioid receptors[42] and IP_3R_3 receptors[15]; however, the role of phosphorylation in the binding of σR1 to these proteins has not been investigated.

Overexpression of σR1 suppressed ER stress-induced activation of the sensor proteins PERK and ATF6, but not IRE1, in an acute model of stress.[15] We asked whether oxidative stress in our in vitro model or metabolic stress in our diabetic retinopathy model would alter expression of ER stress genes and whether the expression levels would be reversed when the cells or mice, respectively were treated with (+)-PTZ. In the in vitro model, we found an increase in BiP gene expression and the expression of the ER stress genes *PERK*, *ATF6*, and *IRE1a*, as well as the downstream genes *ATF4* and *CHOP*. These data suggest that oxidative stress increases expression of several ER stress genes, which is reversed by (+)-PTZ. IP_3Rs govern the release of Ca^{2+} stored within the ER lumen[43]; σR1 stabilizes IP_3R_3 at the mitochondria-associated ER membrane.[15] We examined expression of IP_3R_3 in the in vitro system and found no statistically significant difference in IP_3R_3 mRNA as a consequence of X:XO exposure (with or without (+)-PTZ) over the 24-hour investigation. We did not investigate the binding of σR1 to IP_3R_3 as a consequence of (+)-PTZ. Hayashi and Su[15] explored this in CHO cells; however, they reported that under normal conditions, (+)-PTZ did not affect the association of σR1 with IP_3R_3, but under stress, σR1 had a prolonged association with the IP_3R_3 receptors which could in turn affect the release of Ca^{2+} from the ER. They stated that σR1 does not affect cytosolic Ca^{2+} levels, which is in contrast to the findings of Tchedre et al.[13,14] of robust regulation of intracellular Ca^{2+} by σR1 in glutamate-induced stress of RGC-5 cells. Clearly, the role of σR1 in mediating Ca^{2+} release in the cytosol versus from the ER in retinal neurons warrants further comprehensive analysis.

Given our in vitro findings of alterations in ER stress genes, we asked whether a similar trend would be observed in vivo. Li et al.[23] reported that multiple ER stress markers, including GRP78 (BiP), phospho-IRE1a, and phospho-eIF2a, were significantly upregulated in the retina of *Ins2$^{Akita/+}$* mice, a widely accepted model of complications of diabetes including retinopathy. We isolated neural retinas from *Ins2$^{Akita/+}$* mice that were diabetic and had either received (+)-PTZ over the course of several weeks after diabetes onset, or had not. Several of the same genes that had increased in our in vitro system (*BiP*, *PERK*, *IRE1a*, and *ATF4*) were increased in the in vivo diabetic model and expression levels were similar to control values when the mice had received the (+)-PTZ treatment. It appears that as with the in vitro system, (+)-PTZ attenuates upregulation of ER stress genes in an in vivo model of diabetic retinopathy.

While the role of σR1 in ER stress was supported by our data, we were interested in other genes, not necessarily directly linked to ER stress, with expression that was altered by σR1 ligands in vivo. We analyzed the retinal transcriptome in diabetic mice with a gene microarray. Interesting data emerged showing alterations in diabetic conditions that were reversed with the 4-week (+)-PTZ treatment. Included among the affected genes were *Frzp* and slit homolog 1, genes involved in cell differentiation and axon guidance, respectively.[44,45] Expression of crystallins γ-B and -D was reversed markedly when diabetic mice were treated with (+)-PTZ. These data are noteworthy, given the recent report that proteins of the crystallin superfamily increased dramatically in early diabetic retinopathy.[46] Another gene with altered expression in the *Ins2$^{Akita/+}$* mouse that was reversed by (+)-PTZ treatment was VEGF receptor 1. VEGF (vascular endothelial growth factor) is a molecule involved in numerous physiological functions, including angiogenesis. VEGF bioactivity is transmitted through the binding of specific receptors (VEGF receptor 1, 2, and 3). Our data show an elevation of the receptor in diabetic mice compared with wild-type mice, but a decrease in receptor expression when (+)-PTZ was administered to diabetic animals. Whether an alteration of VEGF receptor 1 is related to retinal structure and function observed when diabetic mice are treated with (+)-PTZ is not known, but will be explored in the future.

TABLE 7. Retinal Gene Expression Difference in 8-Week-Old (+)-PTZ-Treated *Ins2*$^{Akita/+}$ Mice Compared with Nontreated *Ins2*$^{Akita/+}$ Mice

Accession Number	Gene	Function	Change Ratio
Apoptosis			
NM_020507.3	Transducer of ERBB2 (*Tob2*)	Antiproliferation of cells	−2.5
NM_016868	Hypoxia inducible factor 3, alpha subunit (*Hif3a*)	Tumor suppressor	−2.2
NM_019635.2	Serine/threonine kinase 3 (Ste20, yeast homolog) (*Stk3*)	MAPK signaling pathway Apoptosis	−2
NM_009805.4	CASP8 and FADD-like Apoptosis regulator (*Cflar*)	FAS signaling pathway; Apoptosis	−2
NM_013874	D4, zinc and double PHD fingers family 1 (*Dpf1*)	Induction of apoptosis	−2
NM_010562	Integrin linked kinase (*Ilk*)	PTEN dependent cell cycle arrest and apoptosis	−1.9
NM_027318	Zinc finger, HIT domain Containing 1 (*Znhit1*)	Induction of apoptosis	+3.1
NM_001128151	Cat eye syndrome chromosome region, candidate 2 homolog (human) (*Cecr2*)	Induction of apoptosis	+3.2
NM_009822	Runt-related transcription factor 1; translocated to, 1 (cyclin D-related) (*Runx1t1*)	Induction of apoptosis	+3.4
Antiapoptosis			
NM_008142	Guanine nucleotide binding protein (G protein), beta 1 (*Gnb1*)	Cell proliferation	−2.7
NM_078478	Growth hormone inducible Transmembrane protein (*Ghitm*)	Antiapoptosis	−2.5
NM_007906	Eukaryotic translation elongation factor 1 alpha 2 (*Eef1a2*)	Antiapoptosis	−2.4
NM_010480	Heat shock protein 90, alpha (cytosolic), class A member 1 (*Hsp90aa1*)	Act with survivin, cell survival	−2.3
NM_008629	Musashi homolog 1 (Drosophila) (*Msi1*)	Cell proliferation	−2.3
NM_017377	UDP-Gal:betaglcnac beta 1,4-galactosyltransferase, Polypeptide 2 (*B4galt2*)	Cell proliferation	+2.5
NM_008774	Poly A binding protein, cytoplasmic 1 (*Pabpc1*)	Regulation of eif4e and p70 S6 kinase, tumorigenesis	+3.4
NM_134062	Death associated protein kinase 1	Antiapoptosis	+5
NM_009324	T-box 2 (*Tbx2*)	Cell proliferation	+6.4
	Frizzled-related protein (*Frzb*)	Cell differentiation	+7
Cell Cycle			
NM_007840	DEAD (Asp-Glu-Ala-Asp) box polypeptide 5 (*Ddx5*)	Coactivator of p53	−2.3
NM_023268	Quiescin Q6 sulfhydryl oxidase 1 (*Qsox1*)	Cell growth, division Exit cell cycle for cell proliferation	−2
NM_144560	Growth arrest-specific 2 like 1 (*Gas2l1*)	Cell cycle arrest	−1.8
NM_027276	CDC16 cell division cycle 16 homolog (*S. cerevisiae*) (*Cdc16*)	Cell cycle	+1.9
NM_008540	MAD homolog 4 (Drosophila) (*Smad4*)	Cell cycle	+2
NM_007832	Deoxycytidine kinase (*Dck*)	Cell cycle	+2
	Nipped-B homolog (Drosophila) (*Nipbl*)	Cell cycle	+2.3
Neuron/Retina/Eye Development			
NM_024458	Phosducin (*Pdc*)	Expressed at photoreceptor Outer segment	−2.8
NM_011664	Ubiquitin B (*Ubb*)	Loss of Ubb leads to a progressive degenerative	−2.7
NM_001113330	Cone-rod homeobox containing gene (*Crx*)	Disorder affecting neurons	−2.5
NM_053245	Aryl hydrocarbon receptor-interacting	Expressed at photoreceptor	−2.4
NM_007568	Betacellulin, epidermal growth factor family member (*Btc*)	Over expression observed in abnormal retinal layers	−2.3
NM_033610	Synuclein, beta (Sncb)	Highly expressed in Neuronal degeneration	−2
NM_010228.3	Ferritin light chain 1 (*Flt1*)	Null leads to a progressive degenerative disorder affecting neurons	−2
NM_015745	Retinol binding protein 3, interstitial (*Rbp3*)	Expressed in the RPE	−1.9
NM_011698	Lin-7 homolog B (C. Elegans) (*Lin7b*)	Retina development	−1.9
NM_010348	Glutamate receptor, ionotropic, kainate 1 (*Grik1*)	Neuroactive ligand-receptor interaction	+1.8
NM_013625	Platelet-activating factor acetylhydrolase, isoform 1b, beta1 subunit (*Pafah1b1*)	Neuronal migration and development	+2
NM_001008231	Dishevelled associated activator of morphogenesis2 (*Daam2*)	Neuronal cell differentiation	+2
NM_010733	Leucine rich repeat protein 3 (*Lrrn3*)	Regulated expression in neuronal systems	+2
	Zinc finger and BTB domain containing 20 (*Zbtb20*)	Neuronal cell development	+2.4
NM_025985	Ubiquitin-conjugating enzyme E2G 1 (UBC7 homolog, *C. Elegans*) (*Ube2g1*)	ER-associated degradation (ERAD) Null led to a progressive degenerative disorder affecting neurons	+2.7
NM_030708	Zinc finger homeodomain 4 (*Zfhx4*)	Expressed neuronal differentiation	+4
NM_144761	Crystallin, gamma B (*Crygb*)	Eye development; structural constituent of eye lens	+9
NM_007776	Crystallin, gamma D (*Crygd*)	Expressed neuronal differentiation; eye development	+10

(*continues*)

TABLE 7 (*continued*). Retinal Gene Expression Difference in 8-Week-Old (+)-PTZ-Treated *Ins2*$^{Akita/+}$ Mice Compared with Nontreated *Ins2*$^{Akita/+}$ Mice

Accession Number	Gene	Function	Change Ratio
Axon			
NM_015748	Slit homolog 1 (*Drosophila*) (*Slit1*)	Axon guidance	−6
NM_011952	Mitogen-activated protein kinase 3 (*Mapk3*)	Axon guidance	−2
NM_008138	Guanine nucleotide binding protein (G protein), alpha inhibiting 2 (*Gnai2*)	Axon guidance	−1.9
NM_173788	Natriuretic peptide receptor 2 (*Npr2*)	Axon signal pathway	+2
NM_031255	Radial spokehead-like 1 (*Rshl1*)	Cilium	+2
NM_007887	Deubiquitinating enzyme 1 (*Dub1*)	Axon budding	+8
Oxidative Stress/ER Stress			
NM_133779.2	Phosphatidylinositol glycan anchor biosynthesis, class T (*Pigt*)	Induce neuron death by oxidative stress	−4
NM_010431.2	Hypoxia inducible factor 1, alpha subunit (*Hif1a*)	Induce cell death by oxidative stress	−3
NM_007907	Eukaryotic translation elongation factor 2 (*Eef2*)	Increase under oxidative stress	−2
NM_031165.4	Heat shock protein 8 (*Hspa8*)	Indicator of stress of neuron	−2
NM_027988.3	NADPH oxidase organizer 1 (*Noxo1*)	Oxidative stress	−2
NM_011508	Eukaryotic translation initiation factor 1 (*Eif1*)	Increase under oxidative stress	−1.7
NM_023371	Protein (peptidyl-prolyl cis/trans isomerase) NIMA-interacting 1 (*Pin1*)	Decrease under ER stress	+2
NM_001077510	GNAS (guanine nucleotide binding protein, alpha stimulating) complex locus (*Gnas*)	Calcium signaling pathway	+2
Anti Oxidant			
NM_009729.3	Atpase, H+ transporting, lysosomal V0 subunit C (*Atp6v0c*)	Antioxidant	−2
NM_007747	Cytochrome c oxidase, subunit Va (*Cox5a*)	Antioxidant	+3
Calcium Signaling			
NM_009118	Retinal S-antigen (*Sag*)	Calcium ion binding	−3
NM_022980	Regulator of calcineurin 3 (*Rcan3*)	Calcium ion binding	−2
NM_146079	Guanylate cyclase activator 1B (*Guca1b*)	Calcium ion binding	−2
NM_010017	Dystroglycan 1 (*Dag1*)	Calcium ion binding	+2
NM_001077510	GNAS (guanine nucleotide binding protein, alpha stimulating) complex locus (*Gnas*)	Calcium signaling pathway	+2
ECM Regulation			
NM_007984	Fascin homolog 1, actin bundling protein (*Strongylocentrotus purpuratus*) (*Fscn1*)	Actin binding; actin filament binding	+1.9
NM_017402	Rho guanine nucleotide exchange factor (GEF7) (*Arhgef7*)	Regulation of actin cytoskeleton	+1.9
NM_026002.4	Metadherin (*Mtdh*)	Cell junction	+1.9
NM_009931	Collagen, type IV, alpha 1 (*Col4a1*)	Basement membrane; collagen	+2
NM_013592	Matrilin 4 (*Matn4*)	Formation of filamentous networks in the extracellular matrices	+2
NM_023279	Tubulin, beta 3 (*Tubb3*)	Cell communication; gap junction	+2
NM_007993	Fibrillin 1 (*Fbn1*)	Extracellular matrix structural constituent	+2
NM_172544	Neurexin III (*Nrxn3*)	Cell adhesion molecules	+3
Miscellaneous			
NM_194060	Forkhead box O6 (*Foxo6*)	Related to gene regulation	−5
NM_145625	Eukaryotic translation initiation factor 4B (*Eif4b*)	Mtor signaling pathway	−2
NM_029376.2	Spermatogenesis associated glutamate (E)-rich protein 4a (*Speer4a*)	-	+5

In summary, we investigated the mechanism of retinal neuroprotection by the σR1 ligand (+)-PTZ. The results provide insight into the potential use of σR1 ligands for treatment of retinal diseases. The data support the role of σR1 as a molecular chaperone that binds to BiP under stressful conditions and suggest that (+)-PTZ may exert its effects by dissociating σR1 from BiP. We report that as stress in cells increases, phosphorylation of σR1 increases. This posttranslational modification is attenuated when agonists bind to the receptor. Future studies will systematically examine the consequences of disrupting σR1 phosphorylation. The present study also provides the first evidence that (+)-PTZ can mitigate the upregulation of several ER stress genes in diabetic retinopathy. In addition to ER stress genes, our microarray analysis revealed several other genes that are altered in the diabetic state, but that are reversed by σR1 agonists. These data provide fertile areas for future investigation of the mechanism of σR1 neuroprotection.

Acknowledgments

The authors thank Neeraj Agarwal (National Eye Institute, NIH) for providing us with the RGC-5 cell line.

References

1. Hayashi T, Su TP. An update on the development of drugs for neuropsychiatric disorders: focusing on the sigma 1 receptor ligand. *Expert Opin Ther Targets.* 2008;12:45–58.
2. Hayashi T, Su T. The sigma receptor: evolution of the concept in neuropsychopharmacology. *Curr Neuropharmacol.* 2005;3:267–280.

3. Hanner M, Moebius FF, Flandorfer A, et al. Purification, molecular cloning, and expression of the mammalian sigma 1-binding site. *Proc Natl Acad Sci USA.* 1996;93:8072–8077.
4. Kekuda R, Prasad PD, Fei YJ, Leibach FH, Ganapathy V. Cloning and functional expression of the human type 1 sigma receptor (hSigmaR1). *Biochem Biophys Res Commun.* 1996;229:553–558.
5. Seth P, Leibach FH, Ganapathy V. Cloning and structural analysis of the cDNA and the gene encoding the murine type 1 sigma receptor. *Biochem Biophys Res Comm.* 1997;241:535–540.
6. Seth P, Fei YJ, Li HW, Huang W, Leibach FH, Ganapathy V. Cloning and functional characterization of a sigma receptor from rat brain. *J Neurochem.* 1998;70:922–931.
7. Maurice T, Su TP. The pharmacology of sigma-1 receptors. *Pharmacol Ther.* 2009;124:195–206.
8. Katnik C, Guerrero WR, Pennypacker KR, Herrera Y, Cuevas J. Sigma-1 receptor activation prevents intracellular calcium dysregulation in cortical neurons during in vitro ischemia. *J Pharmacol Exp Ther.* 2006;319:1355–1365.
9. Martin PM, Ola MS, Agarwal N, Ganapathy V, Smith SB. The Sigma receptor (σR) ligand (+)-pentazocine prevents retinal ganglion cell death induced in vitro by homocysteine and glutamate. *Brain Res Mol Brain Res.* 2004;123:66–75.
10. Dun Y, Thangaraju M, Prasad P, Ganapathy V, Smith SB. Prevention of excitotoxicity in primary retinal ganglion cells by (+)-pentazocine, a sigma receptor-1 specific ligand. *Invest Ophthalmol Vis Sci.* 2007;48:4785–4794.
11. Smith SB, Duplantier JN, Dun Y, Mysona B, Martin PM, Ganapathy V. In vivo protection against retinal neurodegeneration by the sigma receptor 1 ligand (+)-pentazocine. *Invest Ophthalmol Vis Sci.* 2008;49:4154–4161.
12. Bucolo C, Drago F, Lin LR, Reddy VN. Sigma receptor ligands protect human retinal cells against oxidative stress. *Neuroreport.* 2006;17:287–291.
13. Tchedre KT, Huang RQ, Dibas A, Krishnamoorthy RR, Dillon GH, Yorio T. Sigma-1 receptor regulation of voltage-gated calcium channels involves a direct interaction. *Invest Ophthalmol Vis Sci.* 2008;49:4993–5002.
14. Tchedre KT, Yorio T. Sigma-1 receptors protect RGC-5 cells from apoptosis by regulating intracellular calcium, Bax levels, and caspase-3 activation. *Invest Ophthalmol Vis Sci.* 2008;49:2577–2588.
15. Hayashi T, Su TP. Sigma-1 receptor chaperones at the ER-mitochondrion interface regulate Ca(2+) signaling and cell survival. *Cell.* 2007;131:596–610.
16. Hayashi T, Su TP. Sigma-1 receptors (sigma(1) binding sites) form raft-like microdomains and target lipid droplets on the endoplasmic reticulum: roles in endoplasmic reticulum lipid compartmentalization and export. *J Pharmacol Exp Ther.* 2003;306:718–725.
17. Jiang G, Mysona B, Dun Y, et al. Expression, subcellular localization and regulation of sigma receptor in retinal Müller cells. *Invest Ophthalmol Vis Sci.* 2006;47:5576–5582.
18. Kim I, Xu W, Reed JC. Cell death and endoplasmic reticulum stress: disease relevance and therapeutic opportunities. *Nat Rev Drug Discov.* 2008;7:1013–1030.
19. Malhotra JD, Kaufman RJ. The endoplasmic reticulum and the unfolded protein response. *Semin Cell Dev Biol.* 2007;18:716–731.
20. Oshitari T, Hata N, Yamamoto S. Endoplasmic reticulum stress and diabetic retinopathy. *Vasc Health Risk Manag.* 2008;4:115–122.
21. Ikesugi K, Mulhern ML, Madson CJ, et al. Induction of endoplasmic reticulum stress in retinal pericytes by glucose deprivation. *Curr Eye Res.* 2006;31:947–953.
22. Roybal CN, Yang S, Sun CW, et al. Homocysteine increases the expression of vascular endothelial growth factor by a mechanism involving endoplasmic reticulum stress and transcription factor ATF4. *J Biol Chem.* 2004;279:14844–14852.
23. Li J, Wang JJ, Yu Q, Wang M, Zhang SX. Endoplasmic reticulum stress is implicated in retinal inflammation and diabetic retinopathy. *FEBS Lett.* 2009;583:1521–1527.
24. Yoshioka M, Kayo T, Ikeda T, Koizumi A. A novel locus, Mody4, distal to D7Mit189 on chromosome 7 determines early-onset NIDDM in nonobese C57BL/6 (Akita) mutant mice. *Diabetes.* 1997;46:887–894.
25. Barber AJ, Antonetti DA, Kern TS et al. The *Ins2*^{Akita} mouse as a model of early retinal complications in diabetes. *Invest Ophthalmol Vis Sci.* 2005;46:2210–2218.
26. Gastinger MJ, Kunselman AR, Conboy EE, Bronson SK, Barber AJ. Dendrite remodeling and other abnormalities in the retinal ganglion cells of Ins2^{Akita} diabetic mice. *Invest Ophthalmol Vis Sci.* 2008;49:2635–2642.
27. Wu Z, Bowen WD. Role of sigma-1 receptor C-terminal segment in inositol 1,4,5-trisphosphate receptor activation: constitutive enhancement of calcium signaling in MCF-7 tumor cells. *J Biol Chem.* 2008;283:28198–28215.
28. Dun Y, Mysona B, Van Ells TK, et al. Expression of the glutamate-cysteine (x_c^-) exchanger in cultured retinal ganglion cells and regulation by nitric oxide and oxidative stress. *Cell Tissue Res.* 2006;324:189–202.
29. Dun Y, Duplantier JN, Roon P, Martin P, Ganapathy V, Smith SB. Serine racemase expression and D-serine content are developmentally regulated in retinal ganglion cells. *J Neurochem.* 2008;104:970–978.
30. Krishnamoorthy RR, Agarwal P, Prasanna G. et al. Characterization of a transformed rat retinal ganglion cell line. *Brain Res Mol Brain Res.* 2001;86:1–12.
31. Van Bergen NJ, Wood JP, Chidlow G, et al. Recharacterization of the RGC-5 retinal ganglion cell line. *Invest Ophthalmol Vis Sci.* 2009;50:4267–4272.
32. Schmittgen TD, Livak KJ. Analyzing real-time PCR data by the comparative Ct method. *Nat Protocols.* 2008;3:1101–1108.
33. Borenfreund E, Puerner JA. Toxicity determined in vitro by morphological alterations and neutral red absorption. *Toxicol Lett.* 1985;24:119–124.
34. Ola MS, Martin PM, Maddox D, et al. Analysis of sigma receptor (σR1) expression in retinal ganglion cells cultured under hyperglycemic conditions and in diabetic mice. *Brain Res Mol Brain Res.* 2002;107:97–107.
35. Yamagishi S, Ueda S, Matsui T, Nakamura K, Okuda S. Role of advanced glycation end products (AGEs) and oxidative stress in diabetic retinopathy. *Curr Pharm Design.* 2008;14:962–968.
36. Kowluru RA, Kanwar M. Oxidative stress and the development of diabetic retinopathy: contributory role of matrix metalloproteinase-2. *Free Radic Biol Med.* 2009;46:1677–1685.
37. Kortuem K, Geiger LK, Levin LA. Differential susceptibility of retinal ganglion cells to reactive oxygen species. *Invest Ophthalmol Vis Sci.* 2000;41:3176–3182.
38. Desco MC, Asensi M, Márquez R, et al. Xanthine oxidase is involved in free radical production in type 1 diabetes: protection by allopurinol. *Diabetes.* 2002;51:1118–1124.
39. Maher P, Hanneken A. The molecular basis of oxidative stress-induced cell death in an immortalized retinal ganglion cell line. *Invest Ophthalmol Vis Sci.* 2005;46:749–757.
40. Xu C, Bailly-Maitre B, Reed JC. Endoplasmic reticulum stress: cell life and death decisions. *J Clin Invest.* 2005;115:2656–2664.
41. Ishima T, Nishimura T, Iyo M, Hashimoto K. Potentiation of nerve growth factor-induced neurite outgrowth in PC12 cells by donepezil: role of sigma-1 receptors and IP3 receptors. *Prog Neuropsychopharmacol Biol Psychiatry.* 2008;32:1656–1659.
42. Kim FJ, Kovalyshyn I, Burgman M, Neilan C, Chien CC, Pasternak GW. Sigma1 receptor modulation of G-protein coupled receptor signaling: potentiation of opioid transduction independent from receptor binding. *Mol Pharmacol.* 2010;77:695–703.
43. Wojcikiewicz RJH, Pearce MMP, Sliter DA, Wang Y. When worlds collide: IP_3 receptors and the ERAD pathway. *Cell Calcium.* 2009;46:147–153.
44. Bi Y, Huang J, He Y. et al. Wnt antagonist SFRP3 inhibits the differentiation of mouse hepatic progenitor cells. *J Cell Biochem.* 2009;108:295–303.
45. Plump AS, Erskine L, Sabatier C, et al. Slit1 and Slit2 cooperate to prevent premature midline crossing of retinal axons in the mouse visual system. *Neuron.* 2002;33:219–232.
46. Fort PE, Freeman WM, Losiewicz MK, Singh RS, Gardner T. W. The retinal proteome in experimental diabetic retinopathy: up-regulation of crystallins and reversal by systemic and periocular insulin. *Mol Cell Proteomics.* 2009;8:767–779.